

DIAMETER INCREMENT ESTIMATIONS OF *Pinus brutia* Ten. FORESTS STAND OF DUHOK GOVERNORATE, KURDISTAN REGION, IRAQ

Abdulaziz Jameel Younis^{1,*} and Tariq Kurko Salih¹

¹Department of Forestry, College of Agricultural Engineering Science, University of Duhok, Duhok, Iraq.

*Corresponding author email: abdulaziz.younis@uod.ac

Received: 15 May 2025

Accepted: 25 Jun 2025

Published: 08 Oct 2025

<https://doi.org/10.25271/sjuoz.2025.13.4.1581>

ABSTRACT:

Pinus brutia Ten., a native eastern Mediterranean conifer, is prominent in northern Iraq and has enormous importance in the stability of ecosystems, biodiversity, and landscape protection. This study was conducted on Calabrian pine populations sampled from three ecologically differentiated sites in Duhok Province, Kurdistan Region, Iraq. Fifteen trees were selected, five per site, four of which will be used in a model calibration and one will be used for validation. Partial stem analysis was conducted by extracting cross-sections at breast height diameter. Despite the small sample size, the dataset provided sufficient observations for reliable statistical modeling. A systematic model selection framework was employed, incorporating tests of model assumptions, goodness of fit metrics, residual diagnostics, the Salih index to enhance the precision of Ohtomo's test, R^2 interpretation, the Furnival index, and the Bias percent test. Allometric regression models were developed using STATGRAPHICS Centurion 19 software, and both homogeneous and heterogeneous forms were assessed. A t-test confirmed the reliability of the calibration models. Site-specific equations were derived based on the best-fitting regression forms: a curvilinear model was selected for both Zawita ($Di = 6.2 - 1.2119 \times \ln(D)$) and Atrush ($Di = 14.8 - 2.8561 \times \ln(D)$), while a square root transformation yielded the best fit at Belkef ($Di = 14.1 - 1.7501 \times \sqrt{D}$).

KEYWORDS: Diameter increment estimating, Duhok governorate, *Pinus brutia*, Statistical model

1. INTRODUCTION

Pinus brutia, popularly called Brutia pine or Turkish pine, is a widely dispersed species of conifer in the eastern Mediterranean basin. Its natural range spans over countries like Turkey, Greece, Cyprus, Syria, Lebanon, Iraq, and Iran, where the species grows under variable climatic and topographic conditions (Boydak, 2004). In the Kurdistan Region, *Pinus brutia* has ecological and economic importance. According to Shahbaz (2010), they are considered the most important native coniferous tree species in the region, contributing considerably to the forest cover, biodiversity, and landscape stability. *Pinus brutia* is naturally distributed in Iraq, only in the northern part of Duhok Province, particularly in the mountainous areas of Atrush, Zawita, and Belkef. These places are incredibly steep and rugged, possessing elevations that provide favorable microclimates for the species. The total area covered by *Pinus brutia* in this region exceeds 50,000 hectares, making it one of the most extensive natural coniferous forest types in the country (Shahbaz, 2010).

Morales-Molino *et al.* (2021) state that *Pinus brutia* tolerates various environmental stresses, such as drought, during the hot summer months and cool, wet winters, as it is easily adapted to local Mediterranean-type climates. Therefore, it would be ecologically more suitable for afforestation operations and reforestation projects, especially in degraded or erosion-prone lands. Due to its fast growth, drought resistance, and soil-binding root systems, the species has been widely used in plantation projects involving roadside and slope stabilization

plantings (Shahbaz, 2010; Salih, 2020; Mosa, 2016). The species also provides many ecosystem services such as carbon sequestration, shelter for native fauna, and soil erosion control (Torres *et al.*, 2021). Its wood is also widely used for fuel, construction, and local production; however, sharp practices of sustainable management are required to sustain its ecosystem function and productivity (Beram, 2023).

The diameter increment is defined as the increase in the stem diameter of the tree over a specific period, usually expressed in millimeters or centimeters per annum. The growth rate is influenced by many factors, including environmental conditions, soil quality, species attributes, and pollarding techniques (Forrester *et al.*, 2017; Pretzsch *et al.*, 2022). It is an essential metric in ecological and forestry research, used to evaluate the productivity, health, and capacity of trees to sequester carbon (Bontemps & Esper, 2011; Brienen *et al.*, 2015). Growth of trees and wood production are directly correlated with diameter increment. Greater growth in diameter is beneficial for the forestry business as more timber is provided (Brunner *et al.*, 2015). More carbon is sequestered within larger diameter increments of trees, and that contributes to alleviating climate change. Larger trees take in or store more CO₂ than smaller ones (Pretzsch *et al.*, 2022). Monitoring changes in diameter over time helped elucidate tree health and identify environmental stresses from pests, diseases, or drought (Babst *et al.*, 2019). A trunk with significant diameter growth results in a larger trunk size and increased canopy cover, providing important habitat for a variety

* Corresponding author

This is an open access under a CC BY-NC-SA 4.0 license (<https://creativecommons.org/licenses/by-nc-sa/4.0/>)

of organisms, including insects and birds (Lindenmayer *et al.*, 2012). Diameter growth serves as a scientific forest management tool for harvesting at the best time and encouraging sustainable mechanisms (Amoroso *et al.*, 2017).

Diameter increments and DBH are functionally linked to tree size, with diameter growth rates varying as the tree matures. This is usually modeled with mathematical equations and empirical growth equations in forestry because it is extremely difficult to measure the increment of a diameter in the field. Other factors influencing this phenomenon would include environmental conditions, competition, species characteristics, and site quality (Weiner & Thomas, 1992). The relationship between DBH and increment in diameter is a focal point in the fields of forestry, growth modeling, and ecological research. It has importance in estimating biomass accumulation, modeling tree growth patterns over time, and guiding sustainable forest management action plans (Binkley *et al.*, 2002; Pretzsch *et al.*, 2022; Stephenson *et al.*, 2014). Diameter growth is an important indicator for sustainable forestry practices and is widely used in carbon sequestration studies and in potential future forest yield predicting models (Köhl *et al.*, 2015; Zeide, 1993;).

Mathematical Frameworks:

The variation of diameter increment with diameter at breast height (DBH) is commonly described by different types of equations. The relationship between diameter increment and DBH may be analyzed using a variety of statistical models, i.e., logarithmic, square root, quadratic, reciprocal, and linear regression models. The optimal model is usually based on how

well it fits into the data and how well its growth pattern mimics the biological growth pattern (Pretzsch *et al.*, 2022; Zeide, 1993). The simple linear regression or one of its non-linear forms, such as square root, logarithmic, reciprocal, and quadratic, may illustrate how DBH relates to diameter increment (Binkley *et al.*, 2002; Hondo, 2011; Zeide, 1993;). As nonlinear growth patterns are typical of trees, the power, Chapman-Richards, and reciprocal models or logistic models tend to ensure better data fits (Pretzsch *et al.*, 2022; Stephenson *et al.*, 2014). Generally, the model should also consider the developmental stages of the trees themselves as well as the statistical criteria of the coefficient of determination, Bias percentage test, or Furnival Index (Pienaar & Turnbull, 1973; Weiner & Thomas, 1992). The objective of the study is to assess the relationship between diameter increment and DBH at three locations, i.e., Zawita, Atrush, and Belkef, in the Duhok governorate in the Kurdistan Region of Iraq.

2. MATERIALS AND METHODS

Study Area:

The study investigates Calabrian pines that grow naturally through three different areas in Duhok province in the Iraqi Kurdistan Region. Table 1 has information regarding the geography of the areas studied. Generally, the climate of these areas is arid to semi-arid with cold winters and hot and dry summers. The reduced annual rainfall with high evapotranspiration acts as a significant factor in controlling the vegetation regimes and forest growth dynamics (Peel *et al.*, 2007; Youssef *et al.*, 2019).

Table 1: Geographical data of the study locations.

Locations	Latitude	Longitude	Altitude (m)
Zawita	36.89980556	43.14733333	948 – 782
Atrush	36.85272222	43.35819444	1000 – 950
Belkef	36.86147222	43.35236111	903 – 832

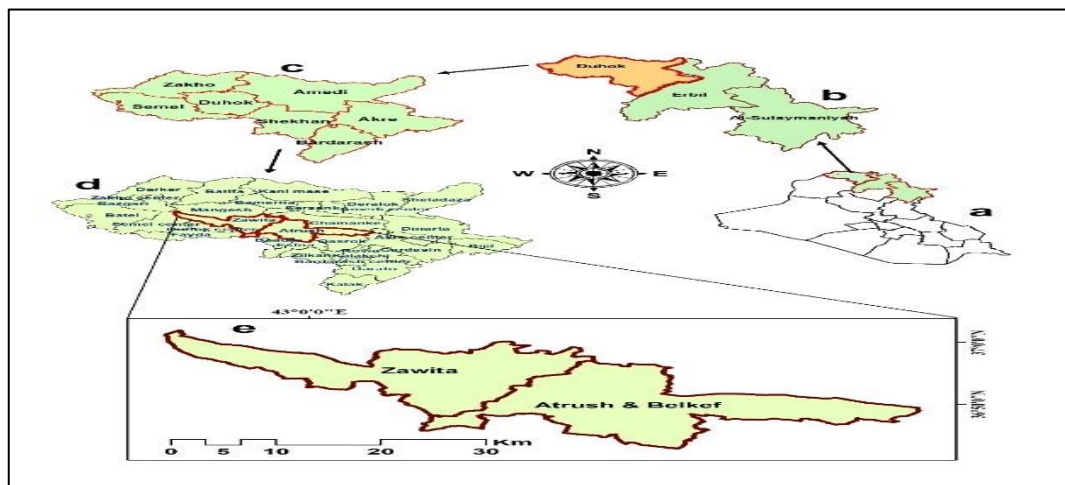


Figure 1: The study area using a geographical map.

Data Collection:

Field Work:

Fifteen trees were deliberately selected from the specified locations, with five trees chosen from each area. Of these, four trees were used for calibration, and one tree was reserved for validation. The selected trees were felled, and cross-sectional discs were extracted at breast height. The thickness of the discs

varied between about 2 and 5 cm. A partial stem analysis was carried out in one specific cross-section of the stem. This method of tree sampling from the stem at one location is recognized by forest research (Akça & Van Laar, 2007; Brack & Wood, 1997; Karukuki, 2002;).

In partial stem analysis, the reconstruction of past diameter increments is achieved by cutting cross-sectional discs from the tree stems. Despite the relatively small sample size of 15 trees

(27-93 years old range), the data set can still provide sufficient observations of 50 in total when considering the yearly increments over time. Each of the sections has several annual growth rings in it, possessing valid data points for regression

analysis (Bräker, 2002; Cook & Kairiukstis, 1990;). This allows tree growth within a specified period to be assessed accurately, even with a smaller number of trees.



Figure 2: Workflow of the field data collection process.

Office Work and Data Compilation:

Office tasks related to this research plan could be classified into three basic phases:

a) Sample Preparation and Enhancement:

This phase includes the refinement of collected stem discs for better visibility of annual growth rings. The samples were sanded first with fine sandpaper for a smooth finish; the clarity of the rings was further enhanced by spraying water on the samples. These refinements are necessary for proper identification and measurement of the rings (Bräker, 2002).

b) Image Preparation and Documentation:

A measurement scale (ruler) is kept beside every prepared sample for reference during calibration. High-definition photographs are obtained using a professional camera under the

same light conditions. Images will be used for references in digital analysis, but clarity and alignment are crucial to ensure trustworthy measurements.

c) Measurement and Data Compilation:

High-resolution images are transferred to a computer for examination using CooRecorder software. The functions of the program include:

1. Measuring the ring width: determining the distance between tree growth rings in two successive years to calculate the annual diameter increment at breast height for each tree stem disc.
2. Exporting the data and statistical processing: All the measured data will be exported to Microsoft Excel for arranging and some preliminary calculations. These final sets of data will be subjected to more rigorous analysis using statistical programs, for example, STATGRAPHICS Centurion, which further allows advanced methods such as regression analysis.

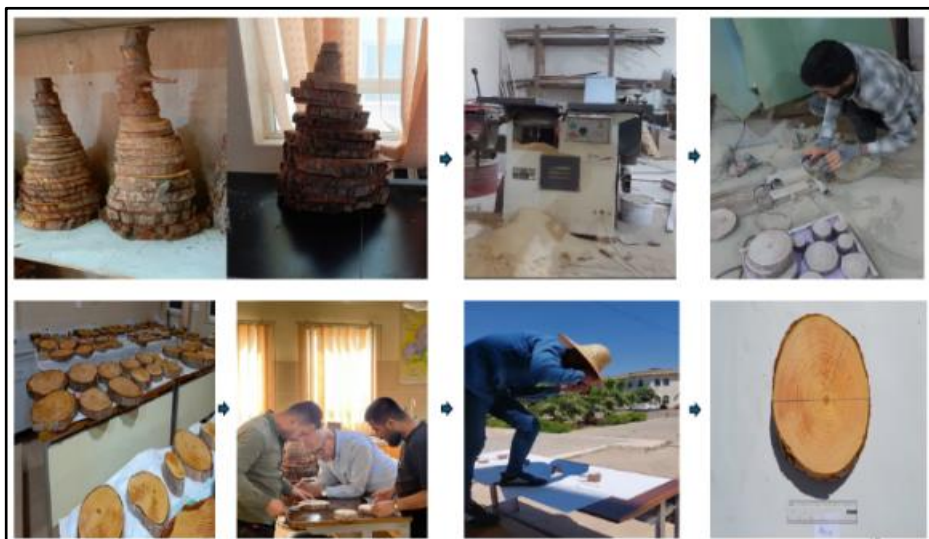


Figure 3: Office workflow for sample analysis and data processing.

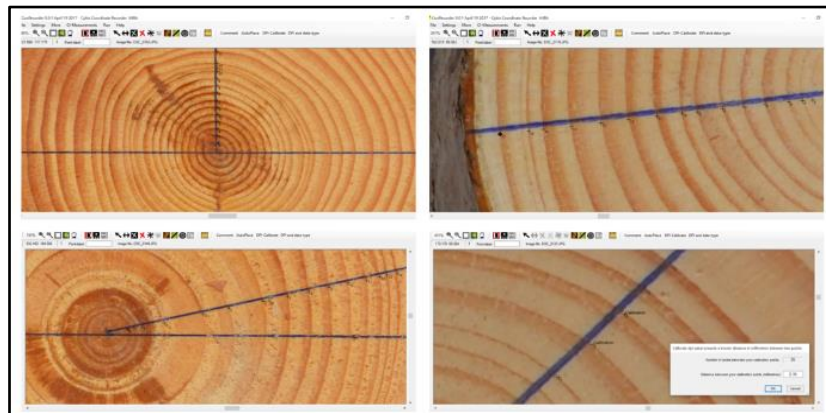


Figure 4: Use of CooRecorder software for extracting tree-ring measurements.

Statistical Description:

It is a vital aspect of any study as it assists in organizing, describing, and interpreting data. In this way, one can summarize data, detect trends, recognize patterns, and make inferences.

Moreover, statistical analysis is critical for understanding relationships between variables, for example, how diameter at breast height influences diameter growth (Moore, 2010; Montgomery & Runger, 2019). The statistical overview for the study locations is presented in Table 2.

Table 2: Summary of statistical data for the studied regions.

Statistics	Zawita Location		Atrush Location		Belkef Location	
	Di (mm)	D (cm)	Di (mm)	D (cm)	Di (mm)	D (cm)
Count	140	140	120	120	142	142
Average	3.04	15.47	7.08	16.54	6.081	23.68
Std.	1.29	6.65	3.09	8.42	3.44	12.86
C.V. %	42.64	43.00	43.65	50.94	56.72	54.30
Minimum	0.84	1.73	1.7	2.59	1.12	1.48
Maximum	6.14	31.18	14.72	31.98	14.04	46.28
Range	5.3	29.45	13.02	29.39	12.92	44.8

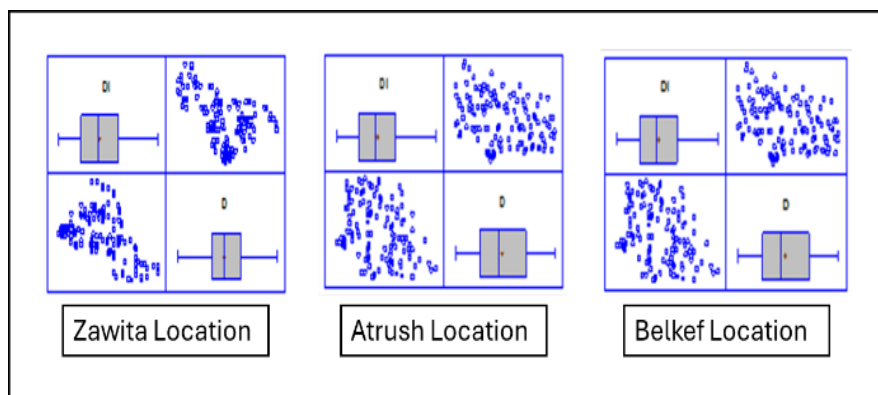


Figure 5: Separate box plots showing the distribution of data for each study location.

Development of the Optimal Model and Statistical Evaluation:

The chosen regression models were implemented based on the method of fixed y-intercept as an approach where the intercept was set according to the maximum and minimum responses obtained for the response variable. In establishing the regression-based most appropriate regression equation that best fits the given research data, the modeling process undertakes two steps:

1) Scatter Diagram Analysis:

The scatter plot is considered a fundamental tool in data analysis; it provides a means by which one can visually test relationships between variables. It aids pattern and trend detection, uncovers outliers, and thereby helps to guide one's choice of regression models. Fields in which scatter diagrams are handy include forest economics, environmental engineering, and forestry research (Montgomery & Runger, 2019; Wooldridge, 2020). Below is the scatter plot representing data from the study locations.

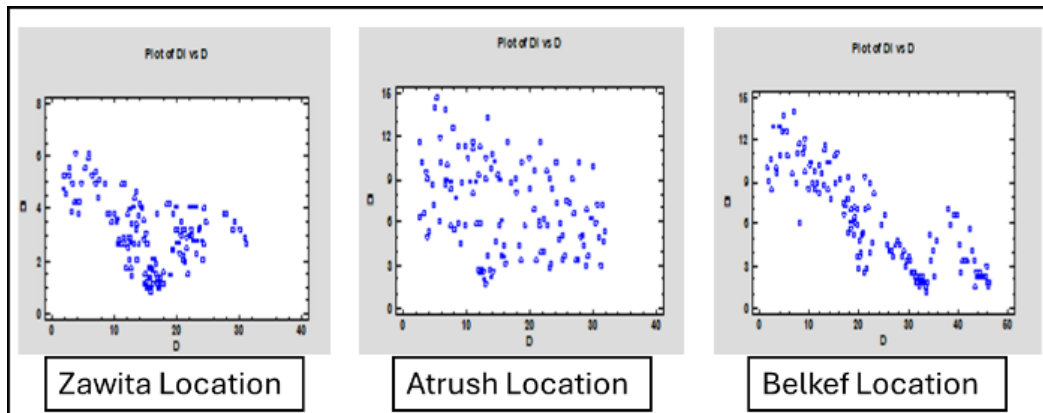


Figure 6: Individual scatter plots illustrating the data distributions for zawita, atrush, and belkef locations.

2) Model Evaluation Criteria and Screening:

A systematic model selection is carried out, aiming at finding the regression model that best describes the data. Model assumptions are to be examined, indicators of goodness-of-fit compared, and residuals investigated. Several statistical tests and evaluation criteria determined the correct regression model for the data. These tests ensured that a model was structurally accurate and provided enough power for prediction. The following is a summary of the screening procedure:

a) Evaluating the Precision of Homogeneous Equations:

The term Homogeneous equations implies regression models in which the dependent variable has the same mathematical form across the various models being compared. For example, suppose all models predict diameter increment as a direct function of diameter at breast height (DBH) without transforming the response variable (for example, using the actual diameter increment rather than its logarithmic or square-root form). In that case, they are referred to as homogenous models. Here, the performance of the different models was compared using a single precision metric.

i) Coefficient of Determination:

It is one of the popular measures used to quantify the amount of variance in the dependent variable accounted for by the model (Neter *et al.*, 1996). It varies between 0 and 1, where a number closer to 1 indicates a better fit. The model with the highest R^2 value is typically selected as the best fit. This measure has been widely used in forestry and ecological research (Abdulqader & Obeyed, 2023; Salih *et al.*, 2023; Younis & Hassan, 2019).

$$\text{Coefficient of determination} = 1 - \frac{SS_{\text{res}}}{SS_{\text{tot}}} \dots\dots\dots (1)$$

Where SS_{res} = a residual sum of square.

SS_{tot} = a total sum of square.

b) Evaluating the Precision of Heterogenous Equations:

Heterogeneous models are those involving different forms of dependent variables. In such cases, two precision metrics are typically used to evaluate model performance more robustly.

i) Test of Furnival Index (FI)

Furnival's Index is a measure of goodness of fit for nonlinear regression models, especially useful in assessing transformations of the dependent variable. Biological and forestry models are often used in cases when tree-growth relationships such as diameter increment against DBH behave in a nonlinear manner (Furnival, 1961). The model with the lowest FI value is deemed

to best fit the data. The metric has been used in various studies (Krishnankutty, 2013; Thapa, 1999; Segura *et al.*, 2006).

$$FI = \frac{\sqrt{\text{Mean square error}}}{\text{Geomean of the first derivative of } y} \dots\dots\dots (2)$$

ii) Salih Index Test:

In 2020, Salih proposed a novel evaluation index that enhances the accuracy and applicability of Ohtomo's test by incorporating multiple key parameters into a single, comprehensive formula. Unlike traditional methods that evaluate only one or two aspects of model performance, Salih's index considers the deviation of four critical component terms: the constants (K), slope (m), coefficient of determination (R^2) from their ideal values, and mean absolute error. This multi-dimensional application provides a more flexible and elaborate estimation of regression model accuracy and appropriateness, mainly in the sense of ecological and forestry studies.

$$\text{Salih Index} = |K - 0| + |1 - m| + |1 - R^2| + MAE \dots\dots\dots (3)$$

The equation, which is assigned to have the least index value, is said to have maximum accuracy, according to this criterion. This evaluation paradigm has been utilized in several academic works, including those of Salih *et al.* (2020), Salih *et al.* (2021), Saeed (2023), and Salih *et al.* (2023).

iii) Bias Percentage Test:

The fittest measure to identify the strength of the bias is the Bias Percentage Test (Abdulqader and Obeyed, 2023), and is equated by the formula:

$$\text{Bias} = \frac{\sum(Y_i - \hat{Y}_i)^2}{\sum Y_i} * 100 \dots\dots\dots (4)$$

Where: Y_i and \hat{Y}_i = actual and estimated value of the i th observation.

The bias percentage indicates how severely the predictions of a model are biased. A value of bias% that is close to zero indicates that the model is an unbiased estimator. In contrast, high positive values imply a biased estimate. Thus, it becomes vital in judging the reliability and predictive performance of regression models.

c) Residual Homogeneity Assessment:

A significant aspect of the regression model being statistically valid, generalizable, and widely acceptable involves having the model show presentable predictive ability over the data. This requires that the residuals, which are expressed as the difference between observed and predicted values, satisfy some general statistical assumptions. Those residuals must have a

standard and independently distributed (NID) specification with zero means and constant variance (σ). It, therefore, protects against systematic model biases, stating that the model errors fall in random distribution from an appropriately specified model. The assurance of validity in any statistical inference should thus depend on whether the above assumptions hold true: accuracy of confidence intervals and soundness in hypothesis testing. Residuals \sim NID (0, σ)

d) Validation of the Selected Regression Model:

Before one begins to use a regression model for predictive purposes, one must first ensure that it is reliable, applicable for the intended task, and validated. This usually involves running the model on an independent dataset that was not involved in calibration. One standard validation procedure consists of creating a separate regression equation based on the validation dataset, in which case the same functional form is applied as for the calibration model. The two models can then be compared on their relative performance to assess the consistency and generalizability of the single model. Within the current study, however, model comparison was carried out using R^2 values, as well as a t-test to capture the differences between calibration and validation models' slope coefficients (see Table 7).

$$t - \text{Test} = \frac{b_1(\text{validation}) - b_1(\text{calibration})}{S_p \sqrt{\frac{1}{n_1} + \frac{1}{n_2}}} \dots \dots \dots \quad (5)$$

$$S_p = \sqrt{\frac{(n_1 - 1)S_1^2 + (n_2 - 1)S_2^2}{n_1 + n_2 - 2}}$$

Where $b_1(\text{validation})$ = slope of the validation model.

$b_1(\text{calibration})$ = slope of calibration model.
 n_1 and n_2 = are the corresponding sample sizes.
 S_p = pooled standard deviation.

3. RESULTS AND DISCUSSION

There are very crucial steps in developing a good regression equation. Starting with data collection and ending with model validation, each step's significance has a bearing on the faithfulness and accuracy of the ultimate model. Here, it is a systematic approach to such key processes and precision metrics as will ensure statistical rigor and model reliability. Such structured methodology is particularly important in scientific research, where the conclusions drawn rely heavily on the quality of statistical modeling. To improve clarity and eliminate any possible redundancy, the methodology of developing regression models has been described in detail only in Part I of this study, as the same methodology was employed in the other sections.

A Compilation of the Developed Regression Equations for the Zawita Site

The software Statgraphics Centurion 19 has been utilized for the construction of a bank of allometric regression models for predicting the key variable. Each model, on the other hand, would fall under one of five groups, based on a particular transformation applied to the dependent (predicted) variables. Out of the 29 models initially developed, only those with the highest accuracy and statistical strength were considered for application in prediction. Ultimately, a set of fifteen models was chosen as the final Zawita representation, as summarized in Table 3.

Table 3: Selected regression models for the Zawita region based on accuracy.

Eq. N.	Equations	R^2
Linear Regression Eq. Models		
1	$D_i = 6.2 - 0.1856*D$	0.837
2	$D_i = 6.2 - 0.8193*sqrt(D)$	0.891
3	$D_i = 6.2 - 1.2119*ln(D)$	0.899
Logarithm Regression Eq. Models		
4	$Ln(D_i) = 1.8245 - 0.0483*D$	0.731
5	$Ln(D_i) = 1.8245 - 0.2134*sqrt(D)$	0.779
6	$Ln(D_i) = 1.8245 - 0.3162*ln(D)$	0.788
Square Root Regression Eq. Models		
7	$\sqrt{D_i} = 2.49 - 0.0465*D$	0.794
8	$\sqrt{D_i} = 2.49 - 0.2053*sqrt(D)$	0.845
9	$\sqrt{D_i} = 2.49 - 0.3039*ln(D)$	0.854
Reciprocal Regression Eq. Models		
10	$D_i = \frac{1}{0.1613 + 0.015*D}$	0.545
11	$D_i = \frac{1}{0.1613 + 0.066*sqrt(D)}$	0.584
12	$D_i = \frac{1}{0.1613 + 0.099*ln(D)}$	0.595
Squared Regression Eq. Models		
13	$D_{i2} = 38.44 - 1.604*D$	0.879
14	$D_{i2} = 38.44 - 7.093*sqrt(D)$	0.938
15	$D_{i2} = 38.44 - 10.483*ln(D)$	0.945

To determine the optimal regression equations, both homogeneity and heterogeneity evaluation were applied. The dependent variables were expressed in various transformed forms across different model groups. From each of the first five groups, the equation with the highest coefficient of determination (R^2)

was selected specifically, equations 3, 6, 9, 12, and 15. The selected linear equations were then subjected to heterogeneity evaluation to assess their robustness and predictive consistency in different datasets further, as shown in Table 4.

Table 4: Determining the best-fitting equation for the study data via heterogeneous evaluation.

Eq. N.	Salih Index	F ¹
3	1.126	1.087
6	1.109	1.812
9	1.107	1.917
12	1.110	3.494
15	1.158	0.475

Further evaluation of the candidate equations was carried out to determine the one that is the best fit. While both the accuracy metrics of Equations 3 and 15 were similar, both were further evaluated with another evaluation called the mathematical limitation test.

Mathematical limitation test:

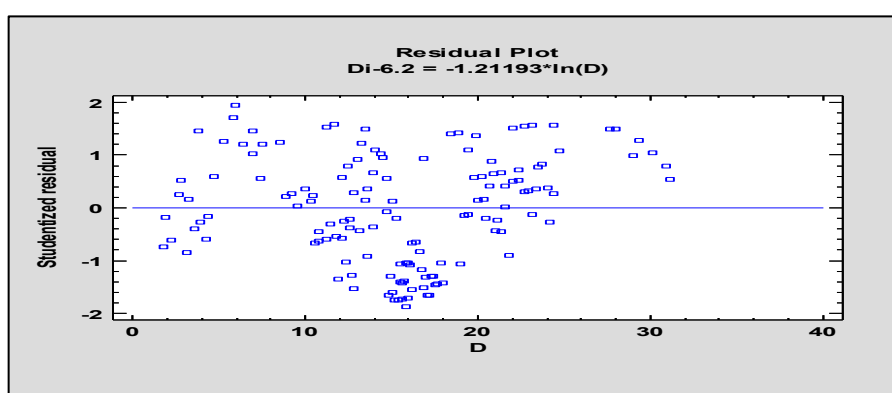
Equations 3 and 15 were tested for mathematical limitations with respect to DBH values, which limit their applicability. The equations were converted into inequalities to identify the point of zero predicted diameter increment or negative increment concerning DBH. In this way, for Equation 3, the inequality $6.2 \leq 1.2119 \ln(D)$ would indicate zero increment at a DBH of 166 cm, beyond the maximum observed, and thereby confirming that it is valid within the parameters of the data set.

Equation 15 led to an inequality of $3.844 \leq 10.483 \ln(D)$, indicating that the diameter increments at the DBH of 39 cm, well

below the maximum of the data set, are zero, and this indicates that it might give biologically unreal values, leading to its being disregarded on account of limited applicability. Equation 3 was selected as the best-fitting model, with justifiable reasons of similar accuracy indices, further yielding favorable m, k, R², and MAE values along with accepted Furnival index values based on standard error.

Homogeneity Test of Residuals for the Selected Equation:

Figure 7 presents a show of residuals versus tree diameter at breast height. Residuals show a random scatter without any visible pattern or trend. This scatter indicates that residuals are normally distributed. The lack of structure in residuals also indicates the appropriateness of the equation. Hence, it indicates that the model fits the data very well, with no significant biases or systematic errors in the regression.

**Figure 7:** The residual distribution of the selected equation for Zawita location.

Established Regression Equations for the Atrush Study Site:

From a range of models with various transformations of dependent and independent variables, fifteen equations were

selected across five groups to constitute the development list for the Atrush site (Table 5).

Table 5: A collection of regression equations developed for the Atrush study area.

Eq. N.	Equations	R ²
Linear Regression Eq. Models		
1	Di = 14.8 - 0.3962*D	0.783
2	Di = 14.8 - 1.8969*sqrt(D)	0.863
3	Di = 14.8 - 2.8561*ln(D)	0.870
Logarithm Regression Eq. Models		
4	Ln (Di) = 2.6946 - 0.0441*D	0.697
5	Ln (Di) = 2.6946 - 0.2100*sqrt(D)	0.762
6	Ln (Di) = 2.6946 - 0.3162*ln(D)	0.768

Squar Root Regression Eq. Models		
7	$\sqrt{D_i} = 3.8471 - 0.0648*D$	0.750
8	$\sqrt{D_i} = 3.8471 - 0.3096*sqrt(D)$	0.822
9	$\sqrt{D_i} = 3.8471 - 0.4661*ln(D)$	0.829
Reciprocal Regression Eq. Models		
10	$D_i = \frac{1}{0.0676 + 0.00585*D}$	0.525
11	$D_i = \frac{1}{0.0676 + 0.0279*sqrt(D)}$	0.574
12	$D_i = \frac{1}{0.0676 + 0.0421*ln(D)}$	0.581
Squared Regression Eq. Models		
13	$D_i^2 = 219.04 - 8.075*D$	0.813
14	$D_i^2 = 219.04 - 38.861*sqrt(D)$	0.905
15	$D_i^2 = 219.04 - 58.561*ln(D)$	0.914

The equations number three, six, nine, twelve, and fifteen were selected from their groups for their highest R^2 values.

Subsequent tests were conducted to identify the most appropriate equation from this set (Table 6).

Table 6: Heterogeneity evaluation results for identifying the optimal equation for the Atrush site.

Eq.	Salih Index	F^I
3	2.763	2.998
6	2.590	4.366
9	2.663	3.825
12	2.387	12.588
15	2.894	0.548

All regression equations accurately predicted diameter increment. However, equations 3 and 15 demonstrated comparable accuracy metrics and were therefore subjected to further evaluation using the Bias percent test. Ultimately, the most effective model that could be chosen was equation 3,

according to the Salih Index, and Furnival Index values as well as Bias percent tests (125.8) against equation 15 (143.5). This bias also showed a more uniform residual distribution among the other candidate models (Figure 8).

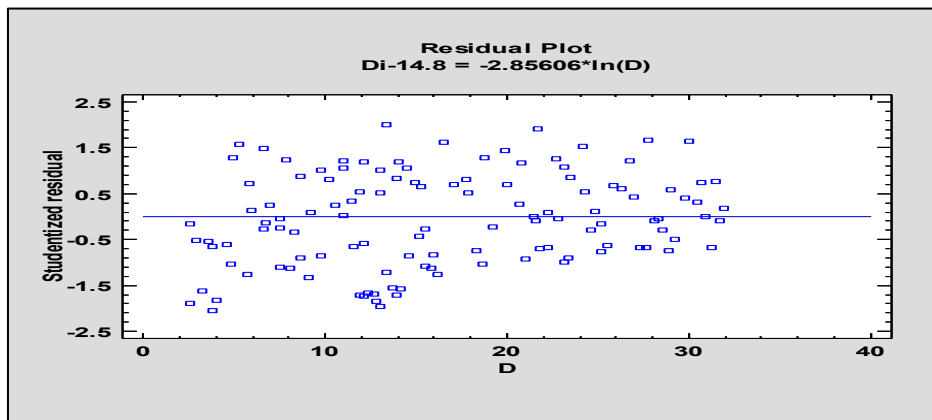


Figure 8: Residual distribution plot for the selected equation at the Atrush site.

A List of Established Regression Equations for the Belkef Site

The same methodology was applied in this section of the study. Among the various models, only 15 equations were

selected to represent the development list for the Belkef site (Table 7).

Table 7: List of regression equations developed for the Belkef site.

Eq. N.	Equations	R^2
Linear Regression Eq. Models		
1	$D_i = 14.1 - 0.3123*D$	0.929
2	$D_i = 14.1 - 1.7501*sqrt(D)$	0.953
3	$D_i = 14.1 - 2.7773*ln(D)$	0.939

Logarithm Regression Eq. Models		
4	$\ln(D_i) = 2.6462 - 0.04277*D$	0.903
5	$\ln(D_i) = 2.6462 - 0.2332*sqrt(D)$	0.877
6	$\ln(D_i) = 2.6462 - 0.3664*ln(D)$	0.847
Squar Root Regression Eq. Models		
7	$\sqrt{D_i} = 3.755 - 0.056*D$	0.927
8	$\sqrt{D_i} = 3.755 - 0.3101*sqrt(D)$	0.926
9	$\sqrt{D_i} = 3.755 - 0.4898*ln(D)$	0.904
Reciprocal Regression Eq. Models		
10	$D_i = \frac{1}{0.0709 + 0.0078*D}$	0.763
11	$D_i = \frac{1}{0.0709 + 0.0412*sqrt(D)}$	0.697
12	$D_i = \frac{1}{0.0709 + 0.0639*ln(D)}$	0.657
Squared Regression Eq. Models		
13	$Di2 = 198.81 - 5.568*D$	0.907
14	$Di2 = 198.81 - 31.826*sqrt(D)$	0.968
15	$Di2 = 198.81 - 50.85*ln(D)$	0.967

Based on the R^2 criterion, only one equation with the highest values were selected from each group for comparison. These competing equations were the second, fourth, seventh, tenth, and

fourteenth on the generated list. Further tests have been conducted on these competing equations to determine the best performing equation (Table 8).

Table 8: Screening criteria for heterogeneous regression models at the Belkef location.

Eq. N.	Salih Index	F^I
2	1.650	1.893
4	1.532	3.097
7	1.640	2.928
10	1.611	8.718
14	Having a mathematical	

Because of some sort of mathematical limitation which produced a negative increase in the diameter increment (DI), equations fourteen and fifteen were left out. The remaining models were subjected to further evaluation by subjecting the total values estimated by each candidate model to comparison with the total from the original dataset. Total values, on the one hand, could be defined as 864 for the actual data and 847, 639,

910, and 671 from the second, fourth, seventh, and tenth equations, respectively. The Second Equation that came closest to the observed value was chosen as the best-fitting model. Compared to the other equations, it had a better Furnival Index and acceptable values regarding the Salih Index parameters. Figure 9 shows the residual distribution for equation 2.

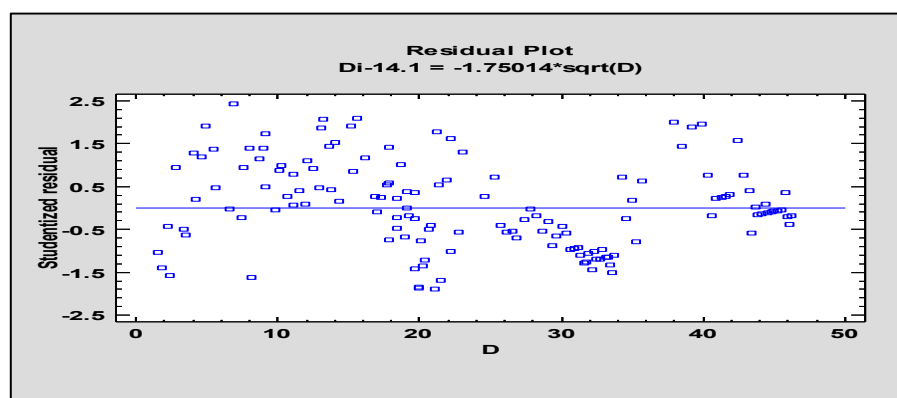


Figure 9: Shows the residual plots of the selected equation for the Belkef location.

Validation:

The table below presents the coefficient of determination (R^2), and the t-test of model comparisons of calibration and

validation applied at the sites of study. Thus, calibration models can confidently be asserted as reliable and consistent in predicting diameter increment and therefore exhibit strong generalizability across various datasets.

Table 9: t-Test and R² results for calibration vs. validation equations by location.

Locations	Equations	b1	R2	Cal. t-Test	Tab. t-Test	Sig.
Zawita	Calibration Eq.	-1.211	0.899	0.939	1.976	Non-sig.
	Validation Eq.	-1.088	0.849			
Atrush	Calibration Eq.	-2.8561	0.870	0.504	1.994	Non-sig.
	Validation Eq.	-3.0395	0.838			
Belkef	Calibration Eq.	-1.7591	0.953	0.312	1.994	Non-sig.
	Validation Eq.	-1.8821	0.903			

The results do not show any important differences between the slopes of the calibration and validation equations, supporting the accuracy and consistency of the calibration models for estimating diameter increments at all sites.

Comparison Between the Selected Regression Model Across Study Sites:

This test was performed by plotting the estimated values of diameter increment for the selected equation across all sites in their original form, corresponding to diameter at breast height (DBH) values ranging from 5 to 55 cm at 2 cm intervals, to evaluate the shape of the resulting curves (Figure 10).

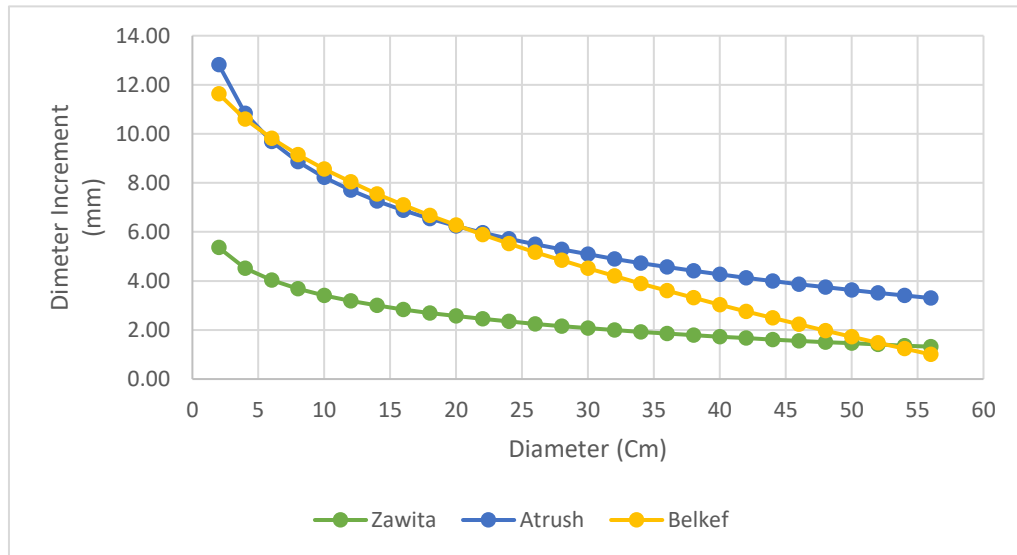


Figure 10: Comparison of diameter increment (mm) vs. tree diameter (cm) at Zawita, Atrush, and Belkef.

The figure depicts quite different growth patterns across the three locations. Among all DBH classes, Zawita (green curve) is consistently the lowest in its diameter growth value. The curve starts very low and progresses upward gradually, indicating a very slow increase in growth as tree size increases.

The Atrush (blue curve) initiates with the highest diameter increase. This is evidenced in its high y-intercept. The curve steadily declines, continuously above the rest, until approximately 30 cm DBH. Beyond that point, it runs almost parallel to Zawita's curve that implies that large trees grow at similar rates in the sites.

The steepest slope is represented by Belkef, indicated in the figure with a yellow line; it reveals the fastest decline in growth increments for increasing diameters at breast height. It intersects the curve of Atrush at around 15 cm and closely approaches that of Zawita at around 50 cm, indicating shifts in their respective growth performance related to time.

Overall, this figure shows that tree growth varies by sites, with Atrush supporting the most vigorous growth in the early stages and Zawita being the slowest across time. These patterns

are more likely attributed to site differences, e.g., in soil quality, moisture, or species composition.

This study has produced two major findings concerning the relationship between diameter increment and tree diameter. First it is the inverse relationship, which implies that as tree diameter increases, the diameter increments decrease. Such growth dynamics, whereby smaller trees grow faster in diameter compared to larger trees, are corroborated by the findings of Larson (1963), Bourian *et al.* (2005), and Biondi and Qeadon (2012). Second, this study showed that using natural logarithm and square root transformations on the predictor variable improved model performance considerably. These transformations explained quite well the non-linearity of the relationship and were similar to the methods used by Söderberg (1986), Edvardsson and Hansson (2015), and Goude (2022) for modeling the growth of Scots pine.

CONCLUSION

This research concludes that a very clear curvilinear relation exists between the diameter increment and the diameter at breast

height (DBH), indicating that growth patterns vary with tree sizes. Nonlinear characteristics of the relationship reveal the complexity of tree growth dynamics and suggest that appropriate transformations must be considered while modeling. Among those transformations tested, the natural logarithm of diameter ($\ln D$) and the square root of diameter (\sqrt{D}) were very effective in improving the fit of the model. Such transformations are quite common in ecological and forestry research to linearize nonlinear relationships and stabilize variance in residuals, thereby improving the robustness and interpretation of regression models.

Furthermore, the results show an inverse relationship. When trees get larger in diameter, their growth in diameter tends to decrease with time. That growth trend can be explained by considering the geometric properties of tree growth: radial growth is spread all around the circumference of the tree. Relative to that circumference, a given amount of radial growth may show a more significant increase in diameter for a small tree because the circumference of a small tree is much smaller in magnitude. Conversely, for larger trees, this growth is spread over an increased circumferential area, giving rise to a relatively reduced increment in terms of diameter. These findings reveal some fundamental biological and physical constraints that must be taken into consideration while dealing with such matters in forest management practices or even in growth model evolution.

Acknowledgments:

The authors sincerely appreciate any contribution that went towards making this research a success. Special thanks to the Directorate of Forests and Rangelands in Duhok (Mr. Kawa, Mr. Hameed, Mr. Faris, and Ms. Nareen) for their invaluable support, as well as the College of Agricultural Engineering Sciences and the Head of the Forestry Department (Dr. Jotyar and Dr. Hishyar) for continued assistance and support.

Ethical Statement:

This study followed all ethical guidelines and institutional regulations that are pertinent to this research. Since it has sensitive, potentially identifiable data, these datasets will not be available publicly. However, access to this data will be provided upon reasonable request to the corresponding author, subject to the necessary approvals by the relevant ethics committee and in accordance with data protection regulations.

Author Contributions:

Authors: Both authors were equally involved in developing the methodology, preparing the original draft, and conducting the review and editing. They have read and approved the final version of the manuscript for publication.

REFERENCES

Abdulqader, H. N., & Obeyed, M. H. (2023). Evaluations of Different Models for Predicting Merchantable Volume of *Pinus Brutia* Ten. in Duhok Governorate. *Science Journal of University of Zakho*, 11(2). <https://doi.org/10.25271/sjuz.2023.11.2.997>

Amoroso, M. M., Daniels, L. D., Baker, P. J., & Camarero, J. J. (Eds.). (2017). *Dendroecology: tree-ring analyses applied to ecological studies* (Vol. 231). Springer. <https://link.springer.com/book/10.1007/978-3-319-61669-8>

Babst, F., Bouriaud, O., Poulter, B., Trouet, V., Girardin, M. P., & Frank, D. C. (2019). "Twentieth century redistribution in climatic drivers of global tree growth." *Science Advances*, 1(1), e1500088. <http://dx.doi.org/10.1126/sciadv.aat4313>

Beram, A. (2023). Improved performance of Brutian pine wood via impregnation with nanoclay. *BioResources*, 18(4), 8076. <DOI: 10.15376/biores.18.4.8076-8089>

Binkley, D., Stape, J. L., Ryan, M. G., Barnard, H. R., & Fownes, J. (2002). "Age-related decline in forest ecosystem growth: an individual-tree, stand-structure hypothesis." *Ecosystems*, 5(1), 58-67. <https://doi.org/10.1007/s10021-001-0055-7>

Biondi, F., & Qeadan, F. (2008). A theory-driven approach to tree-ring standardization: defining the biological trend from expected basal area increment. *Tree-Ring Research*, 64(2), 81-96. <https://doi.org/10.3959/2008-6.1>

Bontemps, J.-D., & Esper, J. (2011). Statistical modelling and RCS detrending methods provide similar results on tree-ring based long-term growth trends. *Dendrochronologia*, 29(2), 143-151. <https://doi.org/10.1016/j.dendro.2010.09.002>

Bourian, D., Guibal, F., & Tessier, L. (2005). Long-term growth trends in temperate forests in southern France. *Forest Ecology and Management*, 214(1-3), 131-145.

Boydak, M. (2004). Silvicultural characteristics and natural regeneration of *Pinus brutia* Ten.—a review. *Plant Ecology*, 171, 153-163. <https://doi.org/10.1023/B:VEGE.0000029373.54545.d2>

Brack and Wood, (1997). Forest Mensuration and Modelling. Available online at [INDEX: Forest Mensuration Resources \(anu.edu.au\)](INDEX: Forest Mensuration Resources (anu.edu.au))

Bräker, O. U. (2002). "Measuring and data processing in tree-ring research—A methodological introduction." *Dendrochronologia*, 20(1-2), 203-216. <https://doi.org/10.1078/1125-7865-00017>

Brienen, R. J. W., et al. (2015). Long-term decline of the Amazon carbon sink. *Nature*, 519(7543), 344-348. <https://doi.org/10.1038/nature14283>

Brunner, I., Herzog, C., Dawes, M. A., Arend, M., & Sperisen, C. (2015). "How tree roots respond to drought." *Frontiers in Plant Science*, 6, 547. <https://doi.org/10.3389/fpls.2015.00547>

Cook, E. R., & Kairiukstis, L. A. (1990). *Methods of Dendrochronology: Applications in the Environmental Sciences*. Springer ISBN 0-7923-0586-8

Edvardsson, J., & Hansson, K. (2015). Dendrochronological potential and growth response of Scots pine to drainage in peatlands. *Scandinavian Journal of Forest Research*, 30(7), 574-582.

Forrester, D. I., et al. (2017). Generalized biomass and leaf area allometric equations for European tree species. *Forest Ecology and Management*, 396, 17-32. <https://doi.org/10.1016/j.foreco.2017.04.011>

Furnival, G. M. (1961). "An index for comparing equations used in constructing volume tables." *Forest Science*, 7(4), 337-341.

Goude, M. (2022). Modeling basal area growth using transformed predictors in boreal forests. *Forest*

Ecosystems, 9, 15. <https://doi.org/10.1186/s40663-022-00357-2>

Hordo, M. (2011). Application of dendroclimatological methods for forest growth modelling. *Eesti Maaülikool*. [ISBN 978-9949-426-99-7](https://doi.org/10.9949-426-99-7)

Karikuki, M., (2002). Height estimation in complete stem analysis using annual radial growth measurements. *Forestry*, 75(1), pp.63-74. <https://doi.org/10.1093/forestry/75.1.63>

Köhł, M., Lasco, R., Cifuentes, M., Jonsson, R., Korhonen, K. T., Mundhenk, P., Neupane, P. R., & Teobaldelli, M. (2015). *Changes in forest production, biomass and carbon: Results from the 2015 Global Forest Resources Assessment*. <https://doi.org/10.1016/j.foreco.2015.05.036>

Krishnankutty, C. N. (2013). Volume tables for trees in home gardens of Kerala. *Indian Forester*, 139(7), 652-657

Larson, P. R. (1963). Stem form development of forest trees. *Forest science*, 9(suppl_2), a0001-42.

Lindenmayer, D. B., Laurance, W. F., & Franklin, J. F. (2012). "Global decline in large old trees." *Science*, 338(6112), 1305-1306. [http://dx.doi.org/10.1126/science.1231070](https://doi.org/10.1126/science.1231070)

Montgomery, Douglas C., and George C. Runger. *Applied statistics and probability for engineers*. John Wiley & Sons, 2019. [ISBN: 978-1-119-40036-3](https://doi.org/10.1111/978-1-119-40036-3)

Moore, D. S. (2010). *The basic practice of statistics*. Palgrave Macmillan. [ISBN-13:978-1-4292-0121-6](https://doi.org/10.1111/978-1-4292-0121-6)

Morales-Molino, C., Arianoutsou, M., Torres Galán, I., & Moreno Rodríguez, J. M. (2021). Ecosystem Services Provided by Pine Forests. https://doi.org/10.1007/978-3-030-63625-8_29

Mosa, W. L. (2016). Forest cover change and migration in Iraqi Kurdistan: a case study from Zawita Sub-district. Michigan State University. <https://doi.org/doi:10.25335/8nae-7e42>

Neter, J., Kutner, M.H., Nachtsheim, C.J. and Wasserman, W., 1996. Applied linear statistical models.

Peel, M. C., Finlayson, B. L., & McMahon, T. A. (2007). Updated world map of the Köppen-Geiger climate classification. *Hydrology and Earth System Sciences Discussions*, 4(2), 439–473. <https://doi.org/10.5194/hessd-4-439-2007>

Pienaar, L. V., & Turnbull, K. J. (1973). *The Chapman-Richards generalization of von Bertalanffy's growth model for basal area growth and yield in even-aged stands*. *Forest Science*, 19(1), 2-22. <https://doi.org/10.1093/forestscience/19.1.2>

Pretzsch, H., M. del Río, F. Giannmarchi, E. Uhl, and R. Tognetti (2022). "Changes of tree and stand growth: review and implications." *Climate-smart forestry in mountain regions* :189-222. [http://dx.doi.org/10.1007/978-3-030-80767-2_6](https://doi.org/10.1007/978-3-030-80767-2_6)

Saeed, H., (2023). The use of complete stem analysis in biometrical studies of Calabrian Pine trees growth in Duhok Governorate region of Iraq. Master's thesis, University of Duhok.

Salih, T. K., (2020). Growth functions modeling of *Quercus aegilops* L. and dendroclimatological Analysis of *Pinus brutia* Ten. In Duhok Governorate (submitted to the Council of the college of agricultural Sciences, Duhok university) PhD dissertation. University of Duhok.

Salih, T. K., Saleem, G. Y., & Younis, A. J. (2023). Comparison between linear and non-linear regression models in the prediction of the height of Gall Oak trees (*Quercus infectoria* Olive.) in Duhok Governorate. [doi:10.1088/1755-1315/1213/1/012118](https://doi.org/10.1088/1755-1315/1213/1/012118)

Salih, T. K., Younis, M. S., & Wali, S. T. (2021, November). Allometric regression equations between diameter growth and age of valonia oak trees grown in Duhok province, Iraq. In International Hasankeyf Scientific Research and Innovation Congress (pp. 557-576).

Segura, M., Kanninen, M., & Suárez, D. (2006). Allometric models for estimating aboveground biomass of shade trees and coffee bushes grown together. *Agroforestry systems*, 68, 143- 150. <https://doi.org/10.1007/s10457-006-9005-x>

Shahbaz S.E., (2010). Trees and Shrubs, afield guide to the trees and shrubs of Kurdistan region of Iraq, Duhok University.

Söderberg, U. (1986). *Funktioner för skogliga produktionsprognosser: Tillväxt och formhöjd för enskilda träd av tall och gran i Sverige* [Functions for forest production forecasts: Growth and form height for individual Scots pine and Norway spruce trees in Sweden]. Swedish University of Agricultural Sciences, Reports of the Forest Research Institute, No. 56.

Stephenson, N. L., Das, A. J., Condit, R., Russo, S. E., Baker, P. J., Beckman, N. G., & Coomes, D. A. (2014). "Rate of tree carbon accumulation increases continuously with tree size." *Nature*, 507(7490), 90-93. [http://dx.doi.org/10.1038/nature12914](https://doi.org/10.1038/nature12914)

Thapa, H. B. (1999). Prediction models for above-ground wood of some fast growing trees of Nepal's eastern Terai. *Banko Janakari*, 9(2), 28-35. DOI: <https://doi.org/10.3126/banko.v9i2.17663>

Torres, I., Moreno, J. M., Morales-Molino, C., & Arianoutsou, M. (2021). Ecosystem services provided by pine forests. *Pines and their mixed forest ecosystems in the Mediterranean Basin*, 617-629. [http://dx.doi.org/10.1007/978-3-030-63625-8_29](https://doi.org/10.1007/978-3-030-63625-8_29)

Van Laar, A. and Akça, A., (2007). *Forest mensuration* (Vol. 13). Springer Science & Business Media. <https://doi.org/10.1007/978-1-4020-5991-9>

Weiner, J., & Thomas, S. C. (1992). "Competition and allometry in three species of tree seedlings." *Ecology*, 73(2), 648-658. [http://dx.doi.org/10.2307/1940771](https://doi.org/10.2307/1940771)

Wooldridge, J. M. (2020). *Introductory Econometrics: A Modern Approach* (7th ed.). Cengage Learning.

YOUNIS, A. J., & HASSAN, M. K. (2019). Assessing volume of *Quercus aegilops* L. trees in Duhok Governorate, Kurdistan Region of Iraq. *Journal of Duhok University*, 22(1), 265- 276. [http://dx.doi.org/10.26682/avuod.2019.22.1.25](https://doi.org/10.26682/avuod.2019.22.1.25)

Youssef, S., Galalaey, A., Mahmood, A., Mahdi, H., & Véla, E. (2019). Wild orchids of the Kurdistan Region areas: A scientific window on the unexpected nature of the north-western Zagros. *Société Méditerranéenne d'Orchidologie*.

Zeide, B. (1993). "Analysis of growth equations." *Forest Science*, 39(3), 594-616. <https://doi.org/10.1093/forestscience/39.3.594>